Oxygen Transfer from Organoelement Oxides to Carbon Monoxide Catalyzed by Transition Metal Carbonyls

Anne M. Kelly, Glen P. Rosini, and Alan S. Goldman*

Contribution from the Department of Chemistry, Rutgers, The State University of New Jersey, Piscataway, New Jersey 08855-0939

Received January 17, 1997[⊗]

Abstract: Solutions of $Rh(PR_3)_2(CO)Cl$ (R = Me, Ph) are found to catalyze the rapid transfer of oxygen from amine oxides or organoselenium oxides to carbon monoxide; however, the rhodium complexes undergo no reaction with the oxides in the absence of added CO. Kinetic studies indicate that the catalytically active species is the CO-substituted complex $Rh(PR_3)(CO)_2Cl$, although it is not present in any observable concentration under the conditions of the reaction. $Ir(PPh_3)_2(CO)_2Cl$ also acts as an efficient catalyst precursor for the same oxygen transfer reactions, although like the rhodium complex it undergoes little or no direct reaction with the oxides. The catalytically active species is again found to be the product of substitution of a ligand (in this case, chloride) by CO: $[Ir(PPh_3)_2(CO)_3]^+$ in either ion-paired or unpaired states. Among substrates with weak E−O bonds (E = N, Se), reactivity correlates with substrate basicity in accord with a transition state having the character of a nucleophilic attack (at carbonyl carbon). Oxides with much stronger E−O bonds, even the highly basic triphenylarsine oxide, are much less reactive; the transition state in this case apparently involves significant E−O bond breaking and is presumably not well modeled as a simple nucleophilic attack. $Pt(Ph_3As)(CO)Cl_2$ was found to act as a good catalyst precursor for deoxygenation of arsine oxide, but this system is apparently very complex and the nature of the catalytically active species has not been elucidated.

The transfer of oxygen from amine oxides to a coordinated CO ligand is a well-known reaction, commonly exploited to remove CO from transition metal carbonyls according to eq 1.[1,2]

$$R_3NO + L_nM(CO) \rightarrow R_3N + \text{“}L_nM\text{”} + CO_2 \qquad (1)$$

Reaction 1 is generally believed to proceed via nucleophilic attack by the amine oxide on the metal carbonyl.[3,4] In this respect the reaction is quite unusual: the amine oxide is acting as a *nucleophilic oxidant* and, conversely, the metal carbonyl is acting as an *electrophilic reductant*.

The deoxygenation of other organoelement oxides (e.g. R_n-EO; E = As, S, Se), as well as oxides such as nitro compounds and organic oxygenates (e.g. epoxides or alcohols), has also been reported, generally involving neutral homoleptic metal carbonyls, particularly $Fe(CO)_5$. As in the case of amine oxides, these deoxygenations are generally stoichiometric in the metal carbonyl.[3,4] However, in comparison with reduction of amine oxides, such reactions are of much greater potential value as synthetic routes to the respective deoxygenated products. If metal carbonyls indeed act as electrophilic reductants, they might be expected to display reactivity and selectivity patterns very different from those of typical electron-rich reductants. It is therefore somewhat surprising that there has been little in the way of systematic searching for deoxygenation reagents of this type, including reagents which are more efficient and/or of broader scope, and in particular, *catalytic* reagents (eq 2).

$$R_nEO + CO \xrightarrow{L_nM(CO)} R_nE + CO_2 \qquad (2)$$

Catalytic deoxygenation of phosphine oxides, for example, is a goal with particular synthetic and industrial importance (eq 2; $R_nE = R_3P$).

Unfortunately, the factors which determine the relative reactivity—especially catalytic reactivity—of a given metal carbonyl (or a given organoelement oxide) are not well understood. In addition to deoxygenations, an understanding of such factors should also be relevant to important industrial reactions such as the water−gas shift (which can be viewed as “deoxygenation of H_2O”):

$$H_2O + CO \xrightarrow{L_nM(CO)} H_2 + CO_2 \qquad (3)$$

Herein we report the efficient catalytic transfer of oxygen from amine and organoselenium oxides to carbon monoxide, using rhodium(I) and iridium(I) carbonyls, and the results of mechanistic studies of these catalyses. Surprisingly, in all of the cases studied, the reactions are found to proceed predominantly via metal carbonyl complexes that are only present as very minor species in solution.

Results and Discussion

In an attempt to conduct the decarbonylation of $Rh(PMe_3)_2(CO)Cl$ (10 mM in toluene), eq 1, we observed no deoxygenation of Me_3NO (0.10 M) even at 90 °C (only very slow catalyst decomposition resulted). This failure to react is in accord with the observation that only metal carbonyls with high CO stretching frequencies[3,4] tend to undergo eq 1 (as well

[⊗] Abstract published in *Advance ACS Abstracts,* June 15, 1997.

(1) Albers, M. O.; Coville, N. J. *Coord. Chem. Rev.* **1984**, *53*, 227.
(2) Luh, T. Y. *Coord. Chem. Rev.* **1984**, *60*, 255.
(3) (a) Alper, H.; Edward, J. T. *Can. J. Chem.* **1970**, *48*, 1543−1549. (b) Alper, H.; Roches, D. D. *Tetrahedron Lett.* **1977**, *48*, 4155−4158. (c) Alper, H. *Pure Appl. Chem.* **1980**, *52*, 607−614. (d) Alper, H. *Pure Appl. Chem.* **1988**, *60*, 35−38. (e) Alper, H.; Sibtain, F. *J. Org. Chem.* **1988**, *53*, 3306−3309.
(4) (a) Shi, Y. L.; Gao, Y. C.; Shi, Q. Z.; Kershner, D. L.; Basolo, F. *Organometallics* **1987**, *6*, 1528. (b) Gao, Y. C.; Shi, Q. Z.; Kershner, D. L.; Basolo, F. *Inorg. Chem.* **1988**, *27*, 191. (c) Shen, J. K.; Gao, Y. C.; Shi, Q. Z.; Basolo, F. *Organometallics* **1989**, *8*, 2144−2147. (d) Shen, J. K.; Gao, Y. C.; Shi, Q. Z.; Rheingold, A. L.; Basolo, F. *Inorg. Chem.* **1991**, *30*, 1868−1873. (e) Shen, J. K.; Gao, Y. C.; Shi, Q. Z.; Basolo, F. *J. Organomet. Chem.* **1991**, *401*, 295−303. (f) Shen, J. K.; Gao, Y. C.; Shi, Q. Z.; Basolo, F. *Coord. Chem. Rev.* **1993**, *128*, 69−88.

S0002-7863(97)00158-3 CCC: $14.00

as attack by other nucleophiles[5−7]). The CO stretching frequency of $Rh(PMe_3)_2(CO)Cl$, 1956 cm^{-1} (toluene), falls below the usual range of such complexes.[3,4]

Surprisingly, however, under an atmosphere of carbon monoxide, oxygen transfer was *catalyzed* by $Rh(PMe_3)_2(CO)Cl$, according to eq 4.

$$R_3NO + CO \xrightarrow{\text{catalyst}} R_3N + CO_2 \qquad (4)$$

The reaction occurred extremely rapidly, even at 0 °C; indeed, preliminary kinetics indicated that the rate-limiting step was dissolution of the sparingly soluble Me_3NO. When a more soluble amine was used, *N*-methylmorpholine *N*-oxide (NMMO), diffusion of CO into solution appeared to be rate limiting.

In view of its failure to react stoichiometrically (eq 1), the observation of any such catalytic activity of $Rh(PMe_3)_2(CO)Cl$ was intriguing. We considered that an understanding of the factors which result in such a high level of catalytic activity might assist us in the development of catalysts for less easily deoxygenated substrates. Accordingly, we have studied the mechanism of this catalysis and related systems which we have developed in the course of this study.

Rhodium-Catalyzed Amine Oxide Deoxygenation. Preliminary kinetic studies indicated that reaction 4 (NMMO/$Rh(PMe_3)_2(CO)Cl$) was inhibited by the presence of added PMe_3. For more detailed kinetic studies, PPh_3 was used instead of PMe_3 in order to avoid complications arising from the volatility of the latter. Accordingly, $Rh(PPh_3)_2(CO)Cl$ (**1**), which was also found to rapidly catalyze eq 4, was used as a catalyst instead of $Rh(PMe_3)_2(CO)Cl$. For both the PPh_3 and PMe_3 complexes, no species other than the bis(phosphine)carbonyl starting materials were detectable (IR and ^{31}P NMR) in solution, either in the presence or in the absence of CO atmosphere and/or added NMMO. Note that in the absence of catalyst no oxygen transfer is observed, even at 90 °C.

The kinetics of reaction 4 catalyzed by **1** were studied in detail. To maintain constant specified pressures of CO and corresponding equilibrium concentrations in solution while CO is being consumed, reaction cells were designed with large ratios of gas/solution volume (ca. 80) and surface area/solution volume (ca. 1.4 cm^2/mL). Aliquots were removed from the reaction cell, the reaction was immediately quenched by purging with argon to remove CO, and the samples were monitored by IR spectroscopy (disappearance of a NMMO band at 1170 cm^{-1}).

Even with rapid magnetic stirring, at 0 °C the rate of reaction 4 under the initial conditions investigated (20 mM NMMO, 1.0 mM **1**, 50 Torr CO) was apparently limited by the rate of CO diffusion into solution; this was evidenced, in the absence of added Ph_3P, by kinetics of NMMO disappearance which were zero-order in **1** and NMMO. Only at low catalyst concentration (0.2 mM) was the reaction rate found to be approximately first order in NMMO, $k = 1.7 \times 10^{-4}$ s^{-1}. However, the addition of Ph_3P significantly inhibited the reaction: for example, in the presence of 0.5 mM Ph_3P, only 40% completion was observed in 20 h. Since this rate is so much slower than observed in the absence of Ph_3P (e.g. 100% completion in 3 h), diffusion of CO into solution was clearly not rate limiting in this time regime. No inhibition resulted from the addition of 2 mM [PPN][Cl] (PPN = Ph_3PNPPh_3); this argues against the likelihood of a mechanism involving dissociation of chloride anion from **1**.

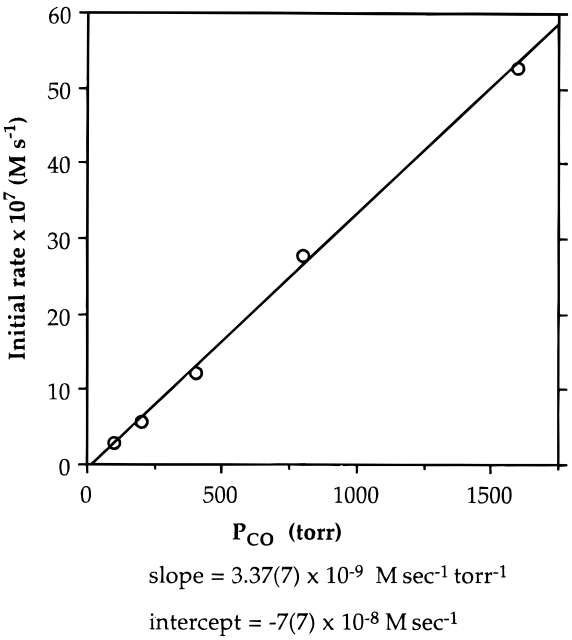

Figure 1. $Rh(PPh_3)_2(CO)Cl$-catalyzed NMMO deoxygenation; CO dependence. [**1**] = 1.0 mM, [Ph_3P] = 1.25 mM, [NMMO] = 20 mM.

When reaction 4 (NMMO) is catalyzed by **1** in the presence of added Ph_3P, plots of the disappearance of NMMO versus time show first-order decay for at least 3 half-lives. When CO pressure is varied, the resulting rates reveal a first-order dependence on P_{CO} (0−1600 Torr) as plotted in Figure 1 ([**1**] = 1.0 mM; [Ph_3P] = 1.25 mM; [NMMO]° = 20 mM; 0 °C; 1,2-dichloroethane solvent; typically monitored for the first 25−30% disappearance of NMMO). Under similar conditions, but varying [Ph_3P] and holding P_{CO} constant at 50 Torr, rates are found to be inverse first order in [Ph_3P] ([Ph_3P] = 0.1−0.8 mM; Figure 2).[8] These results are expressed in eq 5.

$$d[NMMO]/dt = k_5[NMMO][P_{CO}][PPh_3]^{-1} \quad ([\mathbf{1}] = 1.0 \text{ mM}) \qquad (5)$$

$$k_5 = 2.11 \times 10^{-10} \text{ M Torr}^{-1} \text{ s}^{-1}$$

The kinetics indicate a rate-determining transition state of the composition {$Rh(PPh_3)(CO)_2Cl(NMMO)$}, which is most reasonably explained in terms of the following mechanism (R_nE = NMM):

$$Rh(PPh_3)_2(CO)Cl + CO \rightleftharpoons Rh(PPh_3)(CO)_2Cl + PPh_3 \qquad (6)$$

$$Rh(PPh_3)(CO)_2Cl + R_nEO \xrightarrow{k_7\ (\text{r.d.s.})} R_nE + CO_2 + \text{“}Rh(PPh_3)(CO)Cl\text{”} \qquad (7)$$

$$\text{“}Rh(PPh_3)(CO)Cl\text{”} + PPh_3 \rightarrow Rh(PPh_3)_2(CO)Cl \qquad (8)$$

The putative reactive intermediate, $Rh(PPh_3)(CO)_2Cl$, is a known

(5) (a) Darensbourg, D. J.; Darensbourg, M. Y. *Inorg. Chem.* **1970**, *9*, 1691−1694. (b) Darensbourg, M. Y.; Conder, H. L.; Darensbourg, D. J.; Hasday, C. *J. Am. Chem. Soc.* **1973**, *95*, 5919−5924.

(6) Angelici, R. J.; Blacik, L. J. *Inorg. Chem.* **1972**, *11*, 1754−1758.

(7) Dobson, G. R.; Paxson, J. R. *J. Am. Chem. Soc.* **1973**, *95*, 5925−5930.

(8) The intercept of the plot in Figure 2 is apparently nonzero, suggesting a small contribution from a pathway that is not phosphine inhibited. A priori, this could be attributed to direct reaction with the major species, **1**. However, since there is no reaction in the absence of CO, and the intercept of the plot of rate vs P_{CO} is zero (Figure 1), such a pathway appears to involve a dicarbonyl. It may be speculated that this involves the attack of NMMO on a $Rh(PPh_3)_2(CO)_2Cl$, which is known to be present in small concentration (Rosini, G. P.; Goldman, A. S. To be submitted for publication). However, since any such pathway is quite minor, this possibility was not pursued further.

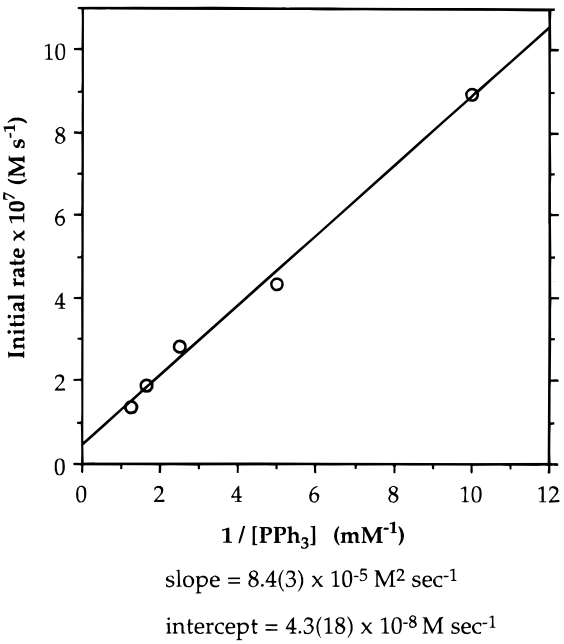

Figure 2. $Rh(PPh_3)_2(CO)Cl$-catalyzed NMMO deoxygenation; $[PPh_3]$ dependence. [**1**] = 1.0 mM, P_{CO} = 50 Torr, [NMMO] = 20 mM.

complex.[9] However, the equilibrium of eq 6 lies too far to the left to be measured directly. Calorimetric measurements[10] reveal that $\Delta H°$ of eq 6 is +7.3 kcal/mol (all species in solution). Treating CO as a standard solute, we assume $\Delta S°$ of eq 6 is approximately zero, and we estimate that under typical reaction conditions the equilibrium constant for eq 6 is ca. 1.4×10^{-6}. The concentration of $Rh(PPh_3)(CO)_2Cl$ is thus quite low under typical reaction conditions, e.g. approximately 9×10^{-9} M under 800 Torr of CO ([CO] = ca. 7.4 mM[11]) in the presence of 1.25 mM PPh_3 and 1.0 mM **1**. The pseudo-first-order rate constant (k_{obs}) for NMMO disappearance under such conditions is 1.39×10^{-4} s^{-1}; therefore, the implied second-order rate constant, k_7, is quite high, ca. 2×10^4 M^{-1} s^{-1} at 0 °C. Consistent with this, the reaction of isolated $Rh(PPh_3)(CO)_2Cl$ with NMMO has thus far proven too fast to obtain reliable kinetics; even at −55 °C, the rate appears to be limited by mixing. Note that the C−O stretching frequencies of $Rh(PPh_3)(CO)_2Cl$, 2093 and 2013 cm^{-1} ($CHCl_3$ solvent), are much greater than that of **1** (1956 cm^{-1}), in accord with the strikingly higher reactivity implied for the dicarbonyl (a factor of at least 10^{13} greater than **1**[12]).

Rhodium-Catalyzed Organoselenium Oxide Deoxygenation. The deoxygenation of di(anisolyl)selenium oxide, An_2SeO, was also found to be catalyzed by **1**.[13]

$$An_2SeO + CO \xrightarrow{\mathbf{1}} An_2Se + CO_2 \quad (9)$$

As was found with amine oxides, no reaction with **1** is observed in the absence of added CO and the deoxygenation under CO is inhibited by added PPh_3;[14] presumably this reaction also proceeds according to eqs 6 and 7 ($R_nE = An_2Se$). Unfortunately, a slow reaction between the selenium oxide and free PPh_3 prevented the acquisition of high-quality kinetic data; for this reason extensive kinetic studies were not conducted. However, a reasonable estimate of the relative rates of **1**-catalyzed NMMO and An_2SeO deoxygenation can be made. For example, under 1600 Torr of CO and in the presence of 1.0 mM **1** and 1.25 mM PPh_3, the first-order rate constant observed for An_2SeO disappearance was 1.16×10^{-5} s^{-1}. (This should be regarded as an upper limit since the oxidation of some PPh_3 would increase the observed rate.) Under the same conditions, the corresponding rate constant for NMMO disappearance is 2.64×10^{-4} s^{-1}. Thus An_2SeO reacts more slowly than NMMO by a factor of ca. ≥20:1. Note that this still implies a very rapid rate of reaction of An_2SeO with $Rh(PPh_3)(CO)_2Cl$, ca. 10^3 M^{-1} s^{-1} at 0 °C.

Amine Oxide Deoxygenation Catalyzed by Solutions of $Ir(PPh_3)_2(CO)_2Cl$. Unlike its rhodium analog, $Ir(PPh_3)_2(CO)Cl$ (Vaska's complex) readily adds CO to give the five-coordinate adduct (**2**)[15] (ca. 99% conversion under 1.0 atm).

$$Ir(PPh_3)_2(CO)Cl + CO \rightleftharpoons Ir(PPh_3)_2(CO)_2Cl\ (\mathbf{2}) \quad (10)$$

Solutions of **2** (actually equilibrium mixtures as indicated in eq 10), like solutions of **1**, were also found to catalyze the rapid deoxygenation of both amine and selenium oxides. Preliminary kinetics suggested, however, that the mechanism was quite different from that of **1**. Most significantly, the rhodium-catalyzed reactions are strongly inhibited by added phosphine, but not by added chloride; the converse, however, was found to be true of the iridium-catalyzed reactions.

Under conditions similar to those described above for the **1**-catalyzed reactions, the rate of **2**-catalyzed deoxygenation of NMMO was decreased significantly by the addition of small quantities of [PPN][Cl] (7-fold decrease at 1.0 mM); above ca. 1 mM [PPN][Cl], however, there was no further inhibition (Figure 3). This behavior implies that in the absence of added chloride the dominant pathway involves a chloride-dissociated intermediate, but at high chloride concentrations one or more alternative pathways are dominant. We conducted kinetic investigations in two regimes: (a) the absence of added chloride and (b) the presence of high concentrations (4−6 mM) of added [PPN][Cl].

The presence of 10 mM Ph_3P in a solution of NMMO (20 mM), **2** (1.0 mM), and [PPN][Cl] (4 mM) under 800 Torr of CO resulted only in a negligible decrease in the observed first-order rate constant for NMMO disappearance (3.8×10^{-4} s^{-1} vs 3.3×10^{-4} s^{-1} in the absence of PPh_3). This may be compared to the **1**-catalyzed system, where the addition of only 0.8 mM Ph_3P decreases k_{obs} by a factor of about 50.

In the presence of added [PPN][Cl] (4 mM), the rate law for **2**-catalyzed deoxygenation of NMMO was found to contain two terms: one which is zero order in P_{CO} and first order in

(9) Gallay, J.; DeMontauzon, D.; Poilblanc, R. *J. Organomet. Chem.* **1972**, *38*, 179−197.

(10) Nolan, S. P. Personal communication, to be submitted for publication.

(11) The solubility of CO in dichloroethane is estimated to be approximately 7.4 mM under 800 Torr of CO, based on values for benzene (7.4 mM, 298°), chlorobenzene (6.4 mM, 293°), and chloroform (8.4 mM, 298°): (a) Linke, W. F. In *Solubilities of Inorganic and Metal Organic Compounds*, 4th ed.; D. Van Nostrand Co.: Princeton, NJ, 1958; Vol. 1, p 453. (b) Gerrard, W. *Solubility of Gases and Liquids*; Plenum Press: New York, 1976; p 141.

(12) This very rough estimate is based on the observed failure of $Rh(PPh_3)_2(CO)Cl$ to react at 90 °C, implying a rate constant of $< 1 \times 10^{-5}$ s^{-1} and $\Delta G^{\neq} \geq 29.7$ kcal/mol. Assuming the hypothetical attack by NMMO would have a reaction entropy between −10 and −30 eu, the enthalpy of the reaction is between 26.1 and 18.8 kcal/mol, respectively. At 0 °C this yields respective rate constants (upper limits) of 5×10^{-11} s^{-1} and 1.4×10^{-9} s^{-1} for the reaction with $Rh(PPh_3)_2(CO)Cl$.

(13) The stoichiometric deoxygenation of selenium oxides by metal carbonyls has been reported previously; see ref 4.

(14) The presence of 4 mM Ph_3P inhibited the rate of disappearance of An_2SeO by a factor of 6; this compares with much more pronounced inhibition of the rate of **1**-catalyzed disappearance of NMMO. This difference may imply that a secondary, minor mechanism for **1**-catalyzed An_2SeO deoxygenation is operative, a pathway that is not inhibited by Ph_3P. Alternatively, the residual disappearance may be due to the direct reaction of Ph_3P with An_2SeO. Since the rates of reaction with Ph_3P appeared irreproducible, these alternatives were not further investigated.

(15) Vaska, L. *Acc. Chem. Res.* **1968**, *1*, 335−344.

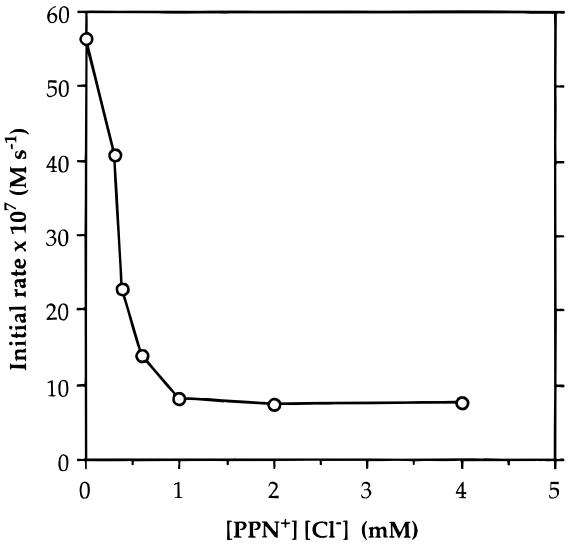

Figure 3. Ir(PPh$_3$)$_2$(CO)Cl-catalyzed NMMO deoxygenation; [PPN][Cl] dependence. [Ir(PPh$_3$)$_2$(CO)Cl] = 1.0 mM, P_{CO} = 800 Torr; [NMMO] = 20 mM.

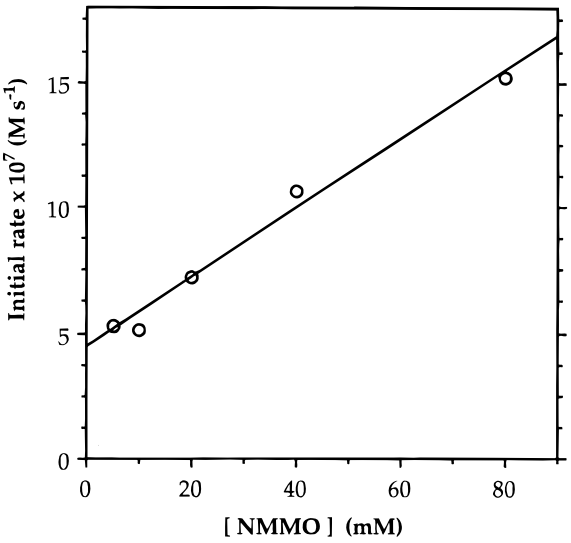

Figure 4. Ir(PPh$_3$)$_2$(CO)Cl-catalyzed NMMO deoxygenation; [NMMO] dependence. [Ir(PPh$_3$)$_2$(CO)Cl] = 1.0 mM; P_{CO} = 800 Torr; 4 mM [PPN][Cl].

[NMMO] and the other first order in P_{CO} and zero order in [NMMO] (Figures 4−6)

$$d[NMMO]/dt = k_{11}[NMMO][\mathbf{2}] + k_{12}[P_{CO}][\mathbf{2}] \quad (11)$$

$$k_{11} = 1.39(10) \times 10^{-2}\ M^{-1}\ s^{-1}$$

$$k_{12} = 7.2(7) \times 10^{-7}\ Torr^{-1}\ s^{-1}$$

The first term implies direct attack by NMMO on **2**, which is consistent with the kinetics of several systems studied by Basolo[4] involving 18-electron carbonyls. The appearance of the second term is much more surprising; it implies a pathway in which the rate-determining step is attack by CO on Ir(PPh$_3$)$_2$(CO)$_2$Cl. (A pre-equilibrium step involving CO addition followed by NMMO attack would be expected to have a [NMMO] term, and assuming the displacement of a ligand, inverse first-order terms in either [Cl$^-$] or [PPh$_3$] would also be required.) A rate-determining associative displacement of PPh$_3$ by CO is, technically, a possible explanation for the k_{12} [P_{CO}] term.

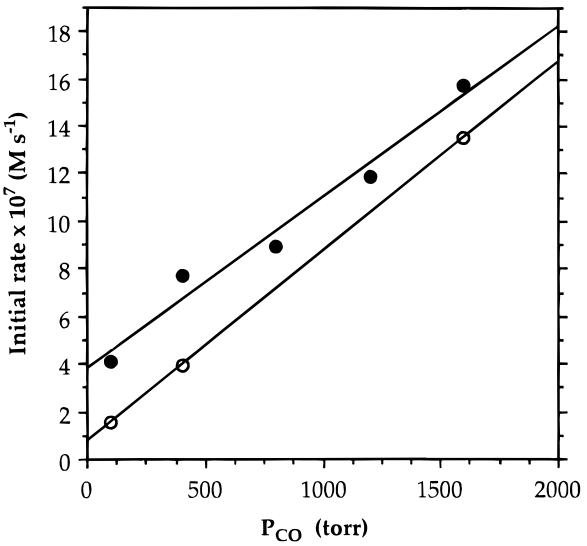

20 mM NMMO slope = 7.2(7) x 10^{-10} M sec^{-1} torr^{-1}

intercept = 3.8(7) x 10^{-7} M sec^{-1}

7 mM NMMO slope = 7.95(2) x 10^{-10} M sec^{-1} torr^{-1}

intercept = 0.77(2) x 10^{-7} M sec^{-1}

Figure 5. Ir(PPh$_3$)$_2$(CO)Cl-catalyzed NMMO deoxygenation; rate vs P_{CO}: (○) 7 mM NMMO; (●) 20 mM NMMO. Line shown is best fit for data with 20 mM NMMO. Slopes are equal within experimental error, while intercepts are clearly different, in accord with eq 11. [Ir(PPh$_3$)$_2$(CO)Cl] = 1 mM; [PPN][Cl] = 4 mM.

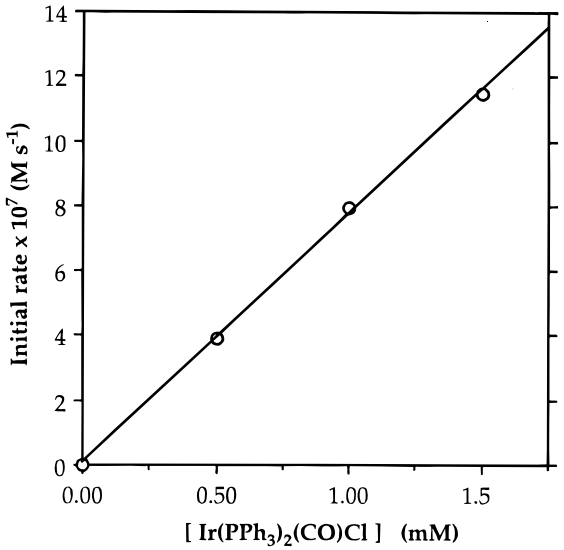

Figure 6. Ir(PPh$_3$)$_2$(CO)Cl-catalyzed NMMO deoxygenation; [Ir(PPh$_3$)$_2$(CO)Cl] dependence. P_{CO} = 800 Torr; 4 mM [PPN][Cl]; [NMMO] = 20 mM.

$$Ir(PPh_3)_2(CO)_2Cl + CO \xrightarrow[\text{r.d.s.}]{-PPh_3} Ir(PPh_3)(CO)_3Cl \xrightarrow{\text{NMMO, fast}} \text{products} \quad (12)$$

However, eq 12 seems implausible. Associative attack on 18-electron complexes is generally not so facile (while deoxygen-

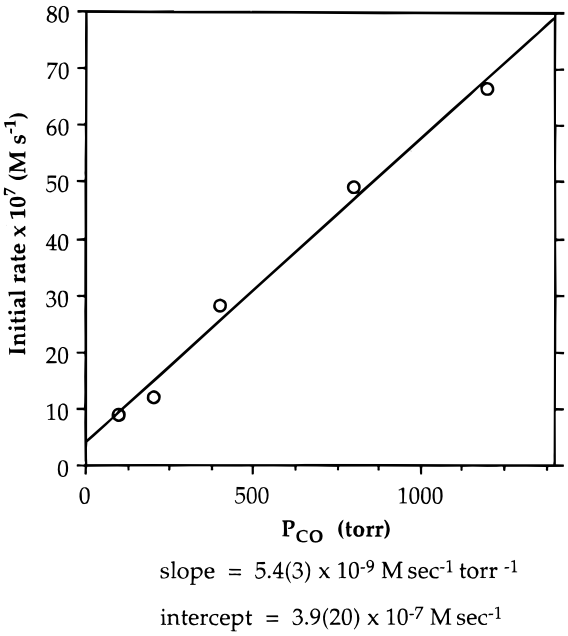

Figure 7. $Ir(PPh_3)_2(CO)Cl$-catalyzed NMMO deoxygenation in the absence of added [PPN][Cl]; P_{CO} dependence. $[Ir(PPh_3)_2(CO)Cl] = 1.0$ mM; [NMMO] = 20 mM.

ation occurs fairly rapidly even at 0 °C). Furthermore, microscopic reversibility arguments would imply that at equilibrium (in the absence of NMMO) a rapid back reaction of $Ir(PPh_3)(CO)_3Cl$ with a minute residual concentration of PPh_3 must also proceed associatively; this is perhaps even less appealing since the required second-order rate constant would be significantly higher.[16] Instead, we propose the following reaction to account for the second term in the kinetic expression of eq 11.

$$Ir(PPh_3)_2(CO)_2Cl \rightleftharpoons \{Ir(PPh_3)_2(CO)_2^+Cl^-\} \xrightarrow[\text{r.d.s.}]{CO} \{Ir(PPh_3)_2(CO)_3^+Cl^-\} \xrightarrow[\text{fast}]{NMMO} \quad (13)$$

Thus the substitution by CO is proposed to proceed "dissociatively", as expected of a five-coordinate Ir(I) system, but because the "dissociated" species is an ion pair, the observed kinetics are those of an associative reaction.

Further evidence for the involvement of the $[Ir(PPh_3)_2(CO)_3]^+$ cation is derived from kinetics obtained in the absence of Cl^- (Figure 7). A plot of rate vs P_{CO} gives a straight line, with an intercept equal to that obtained in the presence of added Cl^- (Figure 5; 20 mM NMMO) but with a much greater slope. The intercept may be attributed to the direct attack by NMMO on **2**, as found in the presence of Cl^-. The greater slope resulting from the absence of added Cl^- is likely to be due to a species in which chloride has been fully dissociated. Indeed, formation of such a cation under CO atmosphere is observed spectroscopically: a small band at 2015 cm^{-1} appears when $Ir(PPh_3)_2(CO)_2Cl$ is placed under 800 Torr of CO (cf. $[Ir(PPh_3)_2(CO)_3][BPh_4]$,[17,18] $\nu_{CO} = 2015$ cm−1).

(16) Note that any such equilibrium lies immeasurably far to the left. Thus this would require a rate constant for associative attack on $Ir(PPh_3)(CO)_3Cl$, by PPh_3, orders of magnitude greater than that required for the forward reaction of CO with $Ir(PPh_3)_2(CO)_2Cl$, since the concentration of PPh_3 is very small but at equilibrium the rates must be equal.

(17) Demming, A. J.; Shaw, B. L. *J. Chem. Soc. A* **1970**, 2705.

(18) Church, M. J.; Mays, M. J.; Simpson, R. N. F.; Stefanini, F. P. *J. Chem. Soc. A* **1970**, 2909−2914.

$$Ir(PPh_3)_2(CO)_2Cl + CO \rightleftharpoons [Ir(PPh_3)_2(CO)_3^+] + Cl^- \quad (14a)$$
2

The intensity of the band at 2015 cm^{-1}, relative to the $Ir(PPh_3)_2(CO)_2Cl$ bands (1982, 1929 cm^{-1}), increases with decreasing concentration of iridium complex (**2**) according to the following equilibrium expression

$$K_{14} = [Ir(PPh_3)_2(CO)_3^+][Cl^-]/[P_{CO}][\mathbf{2}] \quad (14b)$$

$$[Cl^-] = [Ir(PPh_3)_2(CO)_3^+] \quad (14c)$$

$$[Ir(PPh_3)_2(CO)_3^+] = K_{14}^{1/2}[P_{CO}]^{1/2}[\mathbf{2}]^{1/2} \quad (14d)$$

Although the level of precision is low (since the band at 2015 cm^{-1} overlaps with the much more intense band at 1982 cm^{-1}), a plot of the intensity of the 2015 cm^{-1} band vs $[\mathbf{2}]^{1/2}$ gives a straight line. Assuming $\epsilon = 2100$ M^{-1} cm^{-1} (the value calculated for isolated $[Ir(PPh_3)_2(CO)_3][BPh_4]$), the slope is equal to 1.55×10^{-3} $M^{1/2}$, corresponding to $K_{14}^{1/2} = 5.5 \times 10^{-5}$ $M^{1/2}$ $Torr^{-1/2}$.

Addition of [PPN][Cl] results in disappearance of this band as the equilibrium is pushed toward the undissociated species. For example, based on the calculated value of K_{14}, a solution of 1.0 mM **2** under 800 Torr of CO contains 4.9×10^{-5} M $[Ir(PPh_3)_2(CO)_3^+]$; addition of 1.0 mM Cl^- would decrease the concentration by a factor of 20 ($[Ir(PPh_3)_2(CO)_3^+] = 2.4 \times 10^{-6}$ M).

To summarize the above, the kinetic data are all consistent with a relatively slow reaction between $Ir(PPh_3)_2(CO)_2Cl$ and NMMO, and much faster reactions with an ionic complex, $[Ir(PPh_3)_2(CO)_3^+]$, in both ion-paired and unpaired states.

Selenium Oxide Deoxygenation Catalyzed by Solutions of 2. Like NMMO reduction, deoxygenation of An_2SeO catalyzed by **2** is inhibited by added chloride (Table 1) with no further inhibition by chloride observed above ca. 2 mM added [PPN][Cl]. (Also like NMMO reduction, An_2SeO reduction is not significantly inhibited by added phosphine.) In the presence of 6 mM [PPN][Cl] the kinetics are first order in An_2SeO and first order in CO, eq 15 (Table 1, Figure 8).

$$d[An_2SeO]/dt = k_{15}[P_{CO}][An_2SeO]([\mathbf{2}] = 1.0 \text{ mM}) \quad (15)$$

$$k_{15} = 1.52(5) \times 10^{-8}\ s^{-1}\ Torr^{-1}$$

This strongly suggests attack of An_2SeO on the ion pair $[Ir(PPh_3)_2(CO)_3^+][Cl^-]$. (Note that reversible displacement of PPh_3 by CO, followed by attack of An_2SeO, would require an inverse $[PPh_3]$ term, which is not observed. By contrast, reversible displacement of chloride *to give an ion pair* would not yield an inverse $[Cl^-]$ term.)

In the absence of added Cl^-, kinetics consistent with the following rate law are observed (Table 1, Figures 9 and 10):

$$d[An_2SeO]/dt = k_{16}[\mathbf{2}]^{1/2}[P_{CO}]^{1/2}[An_2SeO] + k'_{15}[\mathbf{2}][P_{CO}][An_2SeO] \quad (16)$$

The second term in eq 16 is simply the rate in the presence of added Cl^- ($\{k'_{15}[\mathbf{2}]\} = k_{15}$). In the absence of added Cl^- the first term appears in the rate law and is dominant. Thus, a plot of $\{d[An_2SeO]/dt - k'_{15}[\mathbf{2}][An_2SeO][P_{CO}]\}$ vs $P_{CO}^{1/2}$ gives a straight line with a slope of 9.85×10^{-8} M $Torr^{-1/2}$ s^{-1}, corresponding to $k_{16} = 1.56(7) \times 10^{-4}$ $M^{-1/2}$ $Torr^{-1/2}$ s^{-1} ([**2**] = 1.0 mM, $[An_2SeO]$ = 20 mM; P_{CO} = 100−1600 Torr).[19] Similarly, a plot of $\{d[An_2SeO]/dt - k'_{15}[\mathbf{2}][An_2SeO][P_{CO}]\}$

Table 1. Kinetic Data: An_2SeO Deoxygenation Catalyzed by **2**[a]

	initial rate ($M\ s^{-1}$)	
P_{CO} (Torr)	no added Cl^-	6 mM [PPN][Cl]
100	9.24×10^{-7}	3.33×10^{-8}
400	1.97×10^{-6}	1.33×10^{-7}
800	2.80×10^{-6}	2.65×10^{-7}
1600	4.48×10^{-6}	4.90×10^{-7}

[a] 1 mM $Ir(PPh_3)_2(CO)Cl$, 20 mM An_2SeO, 0 °C, 1,2-dichloroethane solvent.

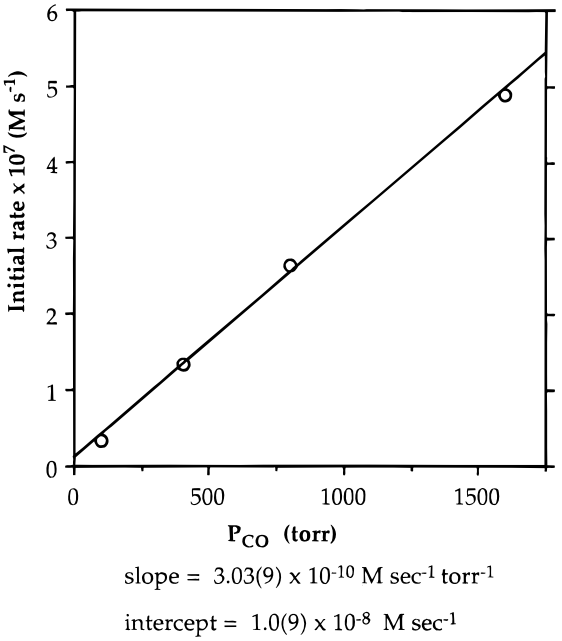

Figure 8. $Ir(PPh_3)_2(CO)Cl$-catalyzed An_2SeO deoxygenation; P_{CO} dependence; 6 mM [PPN][Cl]. $[Ir(PPh_3)_2(CO)Cl] = 1.0$ mM; $[An_2SeO] = 20$ mM.

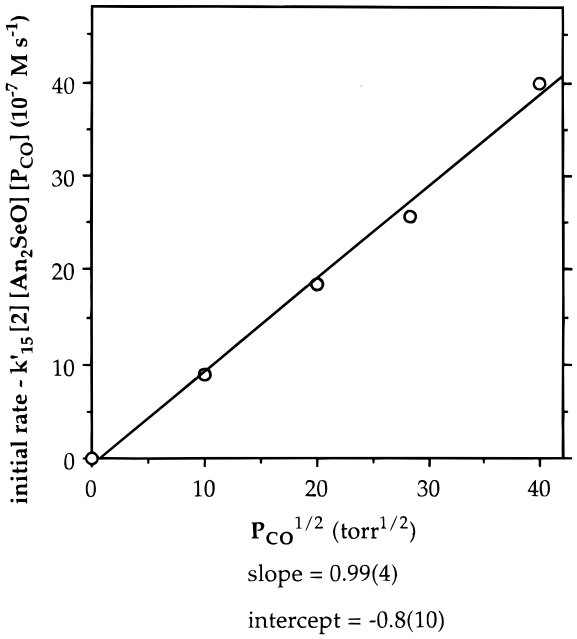

Figure 9. $Ir(PPh_3)_2(CO)Cl$-catalyzed An_2SeO deoxygenation in the absence of added [PPN][Cl]; P_{CO} dependence. $[Ir(PPh_3)_2(CO)Cl] = 1.0$ mM; $[An_2SeO] = 20$ mM. $k_1 = 3.03 \times 10^{-10}$ M s^{-1} $Torr^{-1}$ (obtained from CO dependence with 6 mM [PPN][Cl]). Slope $= 9.85 \times 10^{-8}$ M s^{-1} $Torr^{-1/2} = k_{16}[\mathbf{2}]^{1/2}[An_2SeO]$.

vs $[\mathbf{2}]^{1/2}$ gives a straight line with a slope corresponding to $k_{16} = 1.41(12) \times 10{-}4\ M^{-1/2}\ Torr^{-1/2}\ s^{-1}$ ($P_{CO} = 1600$ Torr, $[An_2SeO] = 20$ mM; $[\mathbf{2}] = 0.25\ {-}1.5$ mM); a log−log plot gives a slope of 0.47(7) (Figure 10).

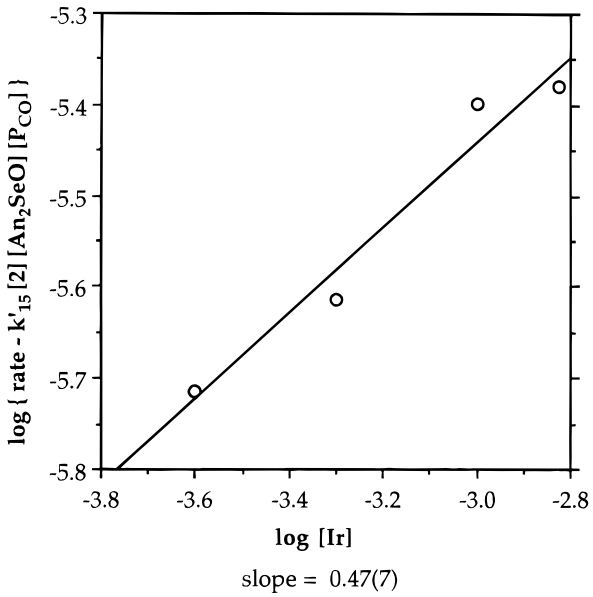

Figure 10. $Ir(PPh_3)_2(CO)Cl$-catalyzed An_2SeO deoxygenation; no added [PPN][Cl]; dependence on log $[Ir(PPh_3)_2(CO)Cl]$. $P_{CO} = 800$ Torr; $[An_2SeO] = 20$ mM.

Scheme 1

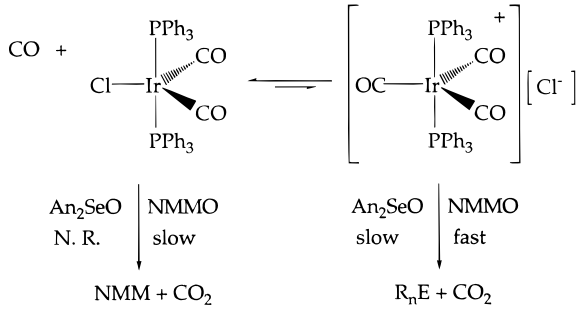

The dominant first term in eq 16 can presumably be attributed to attack by An_2SeO on the unpaired species $[Ir(PPh_3)_2(CO)_3]^+$ (the "free ion"); the half-order terms contained within can be derived from the expression for the equilibrium concentration of the unpaired ion ($K_{1/2}[\mathbf{2}]^{1/2}[P_{CO}]^{1/2}$), eq 14d.

Thus, it can be seen that in spite of the seemingly very different rate laws, the same intermediates proposed for **2**-catalyzed NMMO deoxygenation are operative for **2**-catalyzed An_2SeO deoxygenation. These results are summarized in Scheme 1.

The major difference between the kinetics of the two substrates is that An_2SeO reacts slowly enough with the ionic species (both free ion and ion pair) so that their equilibrium concentrations are maintained, whereas NMMO reacts with the same species rapidly upon their formation. This proposal is subject to an interesting test: deoxygenation of An_2SeO should be inhibited by the presence of NMMO since NMMO should intercept the ionic intermediates. This is found to be the case: A solution of An_2SeO, NMMO, and **2**, shows no disappearance of the An_2SeO for ca. 400 min. At about that time the NMMO

(19) Since the second term in eq 16 is much smaller than the first term, the data fit an equation in which the second term is omitted almost as well as they fit the two-term expression for P_{CO} dependence: $r^2 = 0.991$ vs 0.995 for the one-term and two-term fits, respectively. It should be noted, however, that the smaller term is not an *independent* parameter, but is taken directly from eq 15; therefore, addition of the second term does not inherently lead to a better fit.

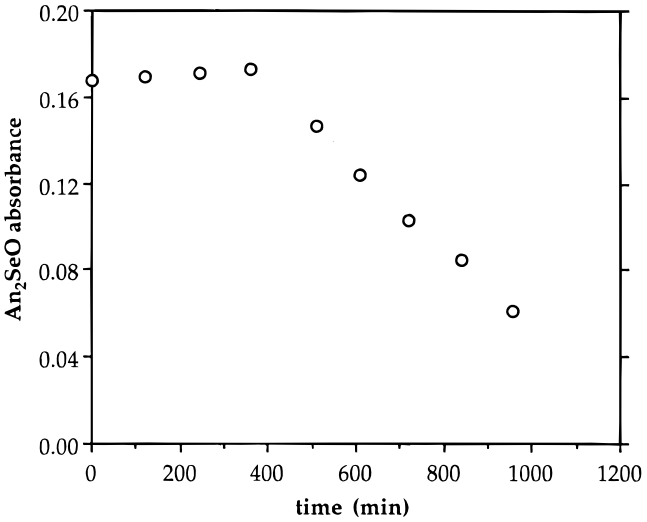

Figure 11. An_2SeO deoxygenation catalyzed by $Ir(PPh_3)_2(CO)Cl$ in the presence of added NMMO. $[Ir(PPh_3)_2(CO)Cl] = 1.0$ mM; [NMMO] = 20 mM; $[An_2SeO] = 20$ mM; $P_{CO} = 800$ Torr; [PPN][Cl] = 6 mM.

is consumed (consistent with **2**-catalyzed NMMO deoxygenation kinetics in the absence of An_2SeO); the An_2SeO then rather abruptly begins to react at the same rate as is observed in the absence of NMMO (Figure 11; $2.7(2) \times 10^{-5}$ s^{-1} vs $2.45(12) \times 10^{-5}$ s^{-1}, respectively).

Spectroscopic observations are also in accord with the proposal that NMMO reacts rapidly with the $[Ir(PPh_3)_2(CO)_3]^+$, whereas An_2SeO reacts slowly enough to allow equilibrium to be maintained. The small equilibrium concentration of $[Ir(PPh_3)_2(CO)_3]^+$ is not observed (2015 cm^{-1}) in a solution of **2** with added NMMO present, whereas the band is decreased only slightly, if at all, by the presence of 20 mM An_2SeO.

Deoxygenation Catalyzed by $[Ir(CO)_3(PPh_3)_2][BPh_4]$. In accord with the proposed role of the $[Ir(CO)_3(PPh_3)_2]^+$ cation in **2**-catalyzed deoxygenation, the isolated tetraphenylborate salt rapidly catalyzed both amine and selenium oxide deoxygenation.

The deoxygenation of An_2SeO catalyzed by 0.15 mM $[Ir(CO)_3(PPh_3)_2][BPh_4]$ in acetone-d_6 proceeded with a pseudo-first-order rate constant of 1.32×10^{-3} s^{-1} at 0 °C. Assuming the rate is first order in catalyst, this corresponds to a second-order rate constant of 8.8 M^{-1} s^{-1}. On the basis of the estimated equilibrium constant for formation of free ion under the conditions of the catalysis, $K_{14}^{1/2} = 5.5 \times 10^{-5}$ $M^{1/2}$ $Torr^{-1/2}$, the second-order rate constant under catalytic conditions could be estimated as 2.6 M^{-1} s^{-1}. We consider the observed and estimated catalytic values to be in excellent agreement considering the level of uncertainty in K_{14} and the differences between the two systems (including solvent and counterion). At −50 °C, the pseudo-first-order rate constant for An_2SeO deoxygenation catalyzed by $[Ir(CO)_3(PPh_3)_2][BPh_4]$ was found to be 1.05×10^{-5} s^{-1} (corresponding to a second-order rate constant of 7.0×10^{-2} M^{-1} s^{-1}). These rate constants (0 and 50 °C) yield the following estimates for the activation parameters: $\Delta H^{\ddagger} = 11.2$ kcal/mol; $\Delta S^{\ddagger} = -13$ eu.[4,20]

Deoxygenation of NMMO (10 mM) catalyzed by $[Ir(CO)_3(PPh_3)_2][BPh_4]$ (0.15 mM) proceeds too fast to measure even at −50 °C. Obviously, the much faster reaction with amine oxide compared with selenide oxide is consistent with the differences in the catalytic kinetics observed for the two substrates. A lower limit of 3×10^{-3} s^{-1} was obtained for the pseudo-first-order rate constant for the amine oxide reaction at −50 °C, corresponding to 1.1×10^3 M^{-1} s^{-1} for a second-order rate constant. Using the entropy value obtained for the selenide oxide reaction (−13 eu), we can estimate an upper limit for $\Delta H^{\ddagger}$ as 6.9 kcal/mol, and a lower limit for the second-order rate constant at 0 °C as 2.4×10^4 M^{-1} s^{-1}.

Relative Reactivities of Different Substrates. The second order rate constants estimated for the reactions of the catalytically active species with NMMO and An_2SeO are shown in Table 2.

Ph_2SeO was found to undergo catalysis by **2** at about 1/3 the rate of An_2SeO. This may be attributed to the greater basicity of An_2SeO. A correlation between oxide reactivity and basicity is observed for the three substrates, NMMO ≫ An_2SeO > Ph_2SeO (Table 3). (Basicity is determined by the shift in the MeOH ν_{O-H} band observed upon hydrogen bonding with R_nEO.[4,22]) It should be noted, however, that the greater electron-donating ability of the An_2SeO aryl groups (relative to Ph_2SeO) presumably results in a very slightly greater Se−O bond strength (though they are the same within the error limits of calorimetry). Further, the N−O bond strength of NMMO is significantly greater than that of the selenium oxides. Thus basicity is clearly the dominant factor affecting the rate of oxygen transfer among these substrates.

The basicity of Ph_3AsO, however, is intermediate between that of NMMO and the selenium oxides; yet it was found to undergo deoxygenation, even at increased temperatures, orders of magnitude less rapidly than either the selenium or amine oxides (*vide infra*). This strong departure from the correlation between basicity and reactivity observed for Ph_3AsO may have significant implications. Presumably the decreased reactivity is due to its much greater E−O bond strength (Table 3). This implies (perhaps not surprisingly) that whereas the transition state for the species with weak E−O bonds is essentially a nucleophilic attack on CO, the transition state for substrates with stronger E−O bonds has much more bond-breaking character and much less nucleophilic attack character. Thus, a *complete* lack of reactivity of Ph_3PO with these catalysts is likely due primarily to its very strong E−O bond (ca. 130 kcal/mol[26−28]); and the correlation with its weak basicity may be largely coincidental. This may be summarized with a hypothetical, qualitative energy diagram (Figure 12): The respective con-

(20) This value of $\Delta S^{\ddagger}$ (−13 eu) falls well within the range of values found by Basolo et al. for related stoichiometric reactions (ref 4d). For example, for the reaction of An_2EO (E = Se, Te) with $Cr(CO)_6$, the values of $\Delta S^{\ddagger}$ were −6.9(5) and −22.9(7) eu for E = Te and Se, respectively.

(21) This value is based on the intercept of Figure 8 (rate vs P_{CO}), which is $1.0(9) \times 10^{-8}$ M s^{-1}; this represents the limits (one standard deviation) of the rate of reaction of An_2SeO with **2**. The upper limit of the second order rate constant is thus 2×10^{-8} M s^{-1}/([**2**][An_2SeO]) = 1×10^{-3} M^{-1} s^{-1} ([**2**] = 1.0 mM; [An_2SeO] = 20 mM).

(22) Nelson, J. H.; Nathan, L. C.; Ragsdale, R. O. *J. Am. Chem. Soc.* **1968**, *90*, 5754.

(23) Riley, D. P. Determined calorimetrically for dimethyldodecylamine *N*-oxide; personal communication.

(24) Nolan, S. P.; Kelly, A.; Goldman, A. S. To be submitted for publication.

(25) Conry, R. R.; Mayer, J. M. *Inorg. Chem.* **1990**, *29*, 4862−4867.

(26) Watt, G. D.; McDonald, J. W.; Newton, W. E. *J. Less-Common Met.* **1977**, *54*, 415−423.

(27) Kirklin, D. R.; Domalski, E. S. *J. Chem. Thermodyn.* **1988**, *20*, 743−754.

(28) The first C−O BDE of CO_2(g) is 127.2 kcal/mol. Reported values for the P−O BDE of Ph_3PO range from 124 ± 4 kcal/mol[26] (in dichloroethane, the solvent used in this study) to 136.6 ± 1.2 kcal/mol (liquid phase).[27] (We have chosen, somewhat arbitrarily, the midpoint of this range for Table 1.) If the true P−O BDE indeed lies within this range, the equilibrium concentrations of CO_2 and Ph_3P, if produced, should be observable. Thus the failure of Ph_3PO to undergo observable deoxygenation is apparently due to kinetics, rather than thermodynamics. However, if the value is at or above the upper limit of reported values (≥138 kcal/mol), the equilibrium may lie too far to the left to be observed. To test this possibility, preliminary attempts to observe the reverse reaction, oxygen transfer from CO_2 to Ph_3P, were conducted with several of the catalyst systems; these gave no measurable quantities of Ph_3PO or CO.

Table 2. Estimated Second Order Rate Constants (M^{-1} s^{-1}), 0 °C[a]

	$Rh(CO)(PPh_3)_2Cl$ (**1**)	$Rh(CO)_2(PPh_3)Cl$	$[Ir(CO)_3(PPh_3)_2]^+$ [a]		$Ir(CO)_2(PPh_3)_2Cl$ (**2**)
ν_{CO} (cm^{-1})	1956	2094, 2013	2074, 2012		1983, 1929
k_{CO} (mdyn/Å)	15.45	17.04	16.69		15.46
		Rate Constants			
NMMO	$<10^{-9}$ [b]	2×10^4	$\gg 2.6$[c]	$>2 \times 10^4$ [d]	1.4×10^{-2}
An_2SeO	$<10^{-9}$ [b]	8×10^2	2.6[c]	8.8[d]	$<10^{-3}$ [e]

[a] 1,2-Dichloroethane solvent unless indicated otherwise. [b] Reference 12. [c] Inferred from the kinetics of **2**-catalyzed An_2SeO deoxygenation; reaction with unpaired ion. [d] Directly measured with use of $[Ir(CO)_3(PPh_3)_2][BPh_4]$ in acetone-d_6. [e] Reference 21.

Table 3. Relative Basicity of Several Oxides as Indicated by IR Determination of H Bonding

compd	rel basicity[a]	E−O BDE (kcal/mol)	ref
NMMO	477	70	23
An_2SeO	294	55	24
Ph_2SeO	271	55	24
Ph_3AsO	351	103	25
Ph_3PO	236	129	26−28

[a] $\Delta\nu_{O-H}$ resulting from hydrogen bonding with MeOH (± 5 cm^{-1}).[4,22]

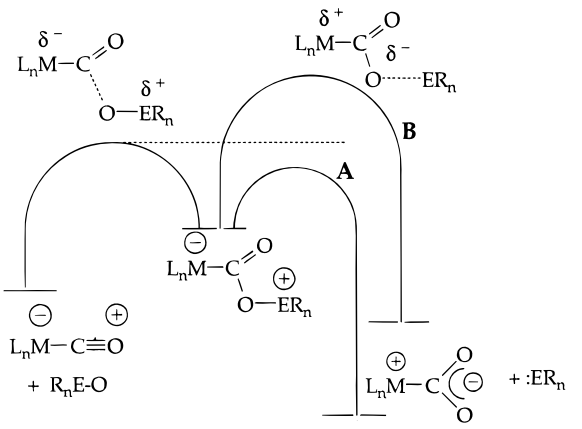

Figure 12. Hypothetical, qualitative energy diagram, comparing reaction pathways for oxides with weak and strong E−O bonds (**A** and **B**, respectively). Note that while the two pathways are analogous the transition states are very different. It is implied that the reactivity of substrates which operate via pathway **A** (e.g. amine oxides) will increase with increasing substrate nucleophilicity, independent of E−O bond strength. Conversely, substrates which operate via pathway **B** are expected to show rates dependent on E−O bond strength and, possibly, independent of nucleophilicity.

tributions of basicity and E−O bond strength have also been discussed by Basolo, particularly in terms of relative entropic and enthalpic factors.[4d]

Rhodium Versus Iridium Systems: Comparisons. A comparison of the different catalyst systems reveals, superficially, little similarity in their kinetics and the implied mechanism. At a fundamental level, however, the similarity between the several reaction mechanisms elucidated is striking. Specifically, in all cases, although the starting materials are carbonyls, a CO-for-ligand (chloride or phosphine) substitution is necessary to give a minor carbonyl species which is key to the major pathway. This behavior has never been reported in the context of nucleophilic attack on CO; indeed, in the most detailed previous mechanistic studies it could not have been operative, since these studies involved homoleptic carbonyls.[4]

This CO-for-ligand substitution pathway is intuitively appealing since the active species is clearly less electron rich than the major species. The discovery of these pathways is encouraging. In many other catalytic reactions of CO, a trade-off involving increased CO pressure is often required: while increased CO may favor some steps, the requirement of a vacant coordination site is disfavored by high concentrations of such a powerfully coordinating ligand. No such trade-off is involved in these systems. These results imply that for many transition metal systems (other than homoleptic carbonyls) high CO pressures (but perhaps no higher than found in common industrial processes) may reveal efficient deoxygenation systems.

For the substrates NMMO and An_2SeO, a correlation between rates and C−O stretching force constants of the metal carbonyls (Cotton−Kraihanzel approximation[29]) is observed (Table 2) in accord with the results of previous studies. This correlation, however, appears to be only approximate at best since complexes **1** and **2** have equal C−O force constants whereas at least 7 orders of magnitude separate the reactivity of these species toward NMMO. This may be attributable to the much greater M−CO BDE of **1** (>ca. 48 kcal/mol)[30] as compared with **2** (10.8 kcal/mol);[15] this would suggest a degree of M−C bond breaking in the transition state. We may also consider the greater nucleophilicity of the fragment $Ir(CO)(PPh_3)_2Cl$ versus $Rh(PPh_3)_2Cl$. The iridium species, which is known to act as a nucleophile,[15,31] may be better able to stabilize a metallocarboxylate-like transition state (see Figure 12). By contrast, although "RhL_2X" fragments bind very strongly to many small molecules,[30,32] the first such CO_2 complex has only recently been observed, and this has been characterized as having an η^2-bound CO_2;[33] therefore even this species is not metallocarboxylate-like.

Finally, we address the potential problem of product inhibition. Many systems conceivably capable of deoxygenating potential substrates such as Ph_3PO might subsequently react with the product, Ph_3P, to give more electron-rich, less reactive species. For example, complex **1**, even if it successfully deoxygenated Ph_3PO, would be inhibited by the Ph_3P thus formed and would therefore not act as a catalyst. The iridium system, however, shows no significant inhibition of reactivity by Ph_3P even at high Ph_3P concentrations. This is presumably due to the fact that both the ground state and active state (tricarbonyl cation) have two phosphine ligands, and that coordination of a third phosphine is prevented by steric effects. This should be a generally applicable principle for these systems: ancillary ligand bulk may prevent inhibition by product without severely inhibiting attack at carbon by the oxide.

Arsine Oxide Deoxygenation. In an effort to explore the scope of the above catalytic systems, particularly with respect

(29) Cotton, F. A.; Kraihanzel, C. S. *J. Am. Chem. Soc.* **1962**, *84*, 4432−4438.
(30) Wang, K.; Rosini, G. P.; Nolan, S. P.; Goldman, A. S. *J. Am. Chem. Soc.* **1995**, *117*, 5082−5088.
(31) Vaska, L.; Werneke, M. F. *Ann. N.Y. Acad. Sci.* **1971**, *172*, 546−562.
(32) Wang, K.; Goldman, A. S.; Li, C.; Nolan, S. P. *Organometallics* **1995**, *14*, 4010−4013.
(33) Vigalok, A.; Ben-David, Y.; Milstein, D. *Organometallics* **1996**, *15*, 1839−1844.

to substrates containing strong E−O bonds, we investigated the catalysts' ability to effect deoxygenation of Ph_3AsO.

Ph_3AsO was not observed to undergo **1**-catalyzed deoxygenation, even after 7 days at 50 °C (800 Torr of CO, 20 mM $Rh(PMe3)_2(CO)Cl$, 200 mM Ph_3AsO). The catalytically active species in the amine and selenium oxide deoxygenations, $Rh(PPh_3)(CO)_2Cl$, when isolated, was not stable in the presence of Ph_3AsO and also afforded no deoxygenation.

Deoxygenation of Ph_3AsO was catalyzed, albeit to a very limited extent, by $[Ir(PPh_3)_2(CO)_3^+]$. A solution of 5 mM $[Ir(PPh_3)_2(CO)_3][BPh_4]$ and 10 mM Ph_3AsO was heated to 50 °C under 800 Torr of CO. After 17 h, 4.7 mM Ph_3As was produced, but only approximately 20% of the $[Ir(PPh_3)_2(CO)_3][BPh_4]$ remained. After 50 h, 5.3 mM of Ph_3As was produced but the catalyst had completely decomposed. CO_2 was detected in the IR spectrum, approximately consistent with the stoichiometry of eq 2.

Platinum Systems. The rhodium- and iridium-based systems described above were relatively amenable to thorough mechanistic analysis. We have, however, also discovered catalysts which are much less amenable to mechanistic study, but which show much greater deoxygenation activity.[34]

We considered that Pd(II) and Pt(II) systems should be much more electrophilic and thus, perhaps, much more reactive than the Ir(I) and Rh(I) systems. In particular, we examined reactivity toward triphenylarsine oxide. $Pt(Ph_3As)(CO)Cl_2$ (**3**) was found to catalyze Me_3NO deoxygenation with rates sufficiently rapid to be limited by gas−solution diffusion. More importantly, at 90 °C, Ph_3AsO deoxygenation was efficiently catalyzed, e.g., 20 turnovers were obtained in 3 h. However, an initial rapid reaction occurred in which **3** was consumed and the solution turned deep green. IR revealed two major types of species in solution. The species present in greatest concentration were (quite surprisingly) platinum carbonyl anions, $[Pt_3(CO)_6]_n^{2-}$, which have a distinctive IR pattern (2065, 1875 cm^{-1}) and a deep green color; these species have been well characterized by Chini and others.[35] In addition to the anions, IR bands of significant intensity were observed at 2045 and 2055 cm^{-1}. While these bands are indicative of carbonyl complexes more electron-rich than the starting material, the frequencies are comparable to those of the catalytically active rhodium and iridium species discussed above. It therefore seems plausible that the bands at ca. 2050 cm^{-1} may be attributable to the active species in this system. Efforts to fully characterize this system and elucidate the mechanism of the catalysis are currently underway.

Quite surprisingly, upon completion of the catalysis and disappearance of Ph_3AsO, all platinum-containing species revert back to the starting complex, **3**, as indicated by both IR and loss of the deep green color. This observation would suggest that a very small equilibrium or steady state concentration of **3** may be present during catalysis; thus, it is possible that **3** is the active species, in accord with our original hypothesis. Mechanistic study of this system is currently underway.

Conclusions. The first examples of the catalytic deoxygenation by CO of the oxides of organoamines, organoselenides, and organoarsines are reported. The mechanism of the amine and selenide oxide reductions has been elucidated, and in all cases the key catalytically active species are formed as the result of substitution of a ligand, either phosphine or halide, by CO. Presumably, the CO-substituted species are less electron-rich than the major species and therefore more susceptible to nucleophilic attack by the oxides. Certainly, the increase in reactivity upon substitution by CO is striking, e.g., a factor of at least 10^{13} upon substitution of a PPh_3 ligand of **1**.

The relative rates of the different substrates suggest that, in the case of species with weak E−O bonds, increased substrate basicity results in increased reaction rate. This has been previously observed in comparing different amine oxides,[4,36] and is in accord with the transition state having the character of a nucleophilic attack on coordinated CO. This relationship between basicity and reactivity holds in spite of the fact that increased basicity can be accompanied by increased E−O bond strength. However, in the case of oxides with strong E−O bonds, even those with high basicity such as Ph_3AsO, deoxygenation is very slow, presumably because the transition state involves cleavage of the E−O bond, and cannot be modeled as the product of a nucleophilic attack. Thus, these results suggest that the development of catalysts for the deoxygenation of substrates with strong E−O bonds may best be accomplished by the design of species in which a metallocarboxylate-like transition state is stabilized.

Experimental Section

General. Solvents were purified by literature methods.[37] $Rh(PMe3)_2(CO)Cl$ was prepared as described previously.[38] $Rh(PPh_3)_2(CO)Cl$ (**1**) was either purchased from Strem Chemicals and used as received or prepared from $Rh(PPh_3)_3Cl$ by the method of Wilkinson.[39] $Ir(PPh_3)_2(CO)Cl$ was purchased from Strem and used as received. Carbon monoxide ("Matheson Purity") was used as purchased from Matheson Gas. NMMO was purchased from Aldrich, vacuum dried, and stored in the glovebox. PPh_3 was recrystallized from hexane. [PPN][Cl] was recrystallized from dichloromethane/ether. Me_3NO was purified by sublimation. Ph_3PO was recrystallized from absolute ethanol. Ph_3AsO was recrystallized from dry benzene and then vacuum dried at 90 °C. *p*-$(CH_3OC_6H_4)_2SeO$ (An_2SeO) was prepared by the method of Basolo[4d] and recrystallized from benzene. Ph_2SeO was prepared by the hydrolysis of Ph_2SeCl_2,[40] and recrystallized from benzene/hexane. All manipulations were performed in a nitrogen-filled glovebox or by using standard Schlenk techniques. IR spectra were taken on a Mattson Cygnus 100 or Mattson Genesis Series FTIR. ^1H NMR spectra were taken on either a Varian VXR-400, a Varian VXR-200, or a Varian Gemini-200 spectrometer. Spectra were referenced to residual solvent peaks. ^{31}P NMR spectra were taken on a Varian VXR-400 NMR spectrometer and were broadband proton decoupled. Spectra were referenced to a PMe_3/toluene-d_8 capillary referenced to 85% H_3PO_4. SigmaPlot (Jandel Scientific) was used for curve-fitting; error values are given in parentheses and represent one standard error.

Measurements of Organoelement Oxide Basicities. An adaptation of a previously reported method was used.[4d,41] A solution of 5 mM MeOH in CCl_4 was prepared. The same solution was used for all measurements. First, 0.1 mmol of the oxide was weighed into a vial in the glovebox. Vials were removed from the glovebox, and 10 mL of the MeOH/CCl_4 solution was added by syringe. The solutions were stirred until the oxide dissolved. (NMMO did not completely dissolve.) Basicities are reported as the shift of the MeOH peak in the IR spectrum from that of the 5 mM MeOH reference sample.

General Procedures for Kinetics. The cell used for these reactions was designed to maximize the rate of CO diffusion into solution. The total volume was approximately 400 mL; dimensions are 17 cm high × 6 cm wide, with the bottom 3 cm tapering at 30° down to a 3 cm

(34) Rosini, G. P.; Joshi, K.; Goldman, A. S. To be submitted for publication.

(35) Longoni, G.; Chini, P. *J. Am. Chem. Soc.* **1976**, *98*, 7225−7231.

(36) Lorkovic, I.; Wrighton, M. S.; Davis, W. M. *J. Am. Chem. Soc.* **1994**, *116*, 6220−8.

(37) Gordon, A. J.; Ford, R. A. In *The Chemist's Companion*; Wiley Interscience: New York, 1972; pp 429−437.

(38) Rosini, G. P.; Boese, W. T.; Goldman, A. S. *J. Am. Chem. Soc.* **1994**, *116*, 9498−9505.

(39) Evans, D.; Osborn, J. A.; Wilkinson, G. *Inorg. Synth.* **1990**, *28*, 79−80.

(40) Rheinbolt, H.; Giesbrecht, E. *J. Chem. Soc.* **1946**, *68*, 2671.

(41) Nelson, J. H.; Nathan, L. C.; Ragsadale, R. O. *J. Am. Chem. Soc.* **1968**, *90*, 5754.

wide flat bottom. The cell was equipped with a Kontes high-vacuum valve and a 9-mm O-ring joint for attachment to a high-vacuum line and a septum inlet for removal of samples by syringe. Reactions were magnetically stirred and run with 5 mL of solution.

All solutions were prepared in a glovebox. For reactions where the CO pressure was less than 800 Torr, the balance was made up with argon. For CO-dependence runs with partial pressures ≤400 Torr, the cell was filled with the desired amount of CO before the addition of the catalyst solution by syringe. This was done to minimize error in the measured CO pressure due to a contribution from the vapor pressure of the dichloroethane. In other cases, the cell was charged with reaction solution in the glovebox, then put through 2 freeze−pump−thaw cycles before the addition of CO. For some reactions, an Ar/CO mixture, purchased from Jersey Welding Supply, was used. This was specified to be 6.51% CO, which affords a partial pressure of 52 Torr of CO at 800 Torr.

Kinetics: Reaction of 1 and NMMO. In the glovebox, 2.5 mL of 2 mM $Rh(PPh_3)_2(CO)Cl$ in dichloroethane was measured into the cell. A Ph_3P stock solution and dichloroethane were added to give a total volume of 4 mL. Following the addition of CO, the cell was placed in an ice−water bath and stirred for approximately 10 min. One milliliter of 100 mM NMMO in dichloroethane was then added by syringe. After approximately 30 s the first sample was withdrawn, immediately syringed into an argon-purged vial with a septum cap, and purged with argon at 0 °C for 15 s. Each sample was then either immediately analyzed by IR spectroscopy, or held at −78 °C for later analysis.

Analysis of NMMO/NMM by IR spectroscopy. An IR solution cell with a 0.5 mm path length and KBr plates was used. A reference spectrum was subtracted from each spectrum: dichloroethane for reactions without added Ph_3P, or a dichloroethane solution of Ph_3P of the same concentration as that of the kinetic run. For the kinetic data, NMMO and the product 4-methylmorpholine (NMM) were quantified by their respective absorbances at 1170 and 1144 cm^{-1}. Because there is a small interference from solvent subtraction at ca. 1144 cm^{-1}, data from the disappearance of NMMO at 1170 cm^{-1} were used for the rate constant calculations. Absorbances were measured by drawing a baseline between approximately 1210 and 910 cm^{-1} and measuring the net absorbance at 1169.6 cm^{-1}. In most cases, the disappearance of approximately the first 25−30% of the NMMO was followed.

Control Reaction: $Rh(PPh_3)_2(CO)Cl$ and NMMO. In the standard reaction cell, 2 mL of 0.2 mM $Rh(PPh_3)_2(CO)Cl$ (4×10^{-4} mmol) in dichloroethane was added to 0.4 mL of 100 mM NMMO (4×10^{-2} mmol). No CO was added to this solution. After 1.5 h at room temperature, no CO_2 was detected ($\nu_{asym} = 2340$ cm^{-1}), and there was no decrease in the absorbance for NMMO at 1170 cm^{-1}. No NMM was produced, determined by zero absorbance at 1144 cm^{-1}. After approximately 5 h, the solution began to turn brown, accompanied by a decrease in the NMMO absorbance; however, no CO_2 or NMM was detected.

Analysis of the Reaction Products by ^1H NMR Spectroscopy. To verify the identity of the product 4-methylmorpholine (NMM), the catalytic reaction was run in acetone-d_6. The sole product was NMM (δ 2.17 (s, 3 H), 2.276 (br s, 4 H), 3.56 (t, 4 H)) as determined by comparison with a standard purchased from Aldrich. There was no evidence of unreacted NMMO: δ 2.82 (d, $J = 11$ Hz, 2H), 3.11 (s, 3 H), 3.43 (td, $J = 9.6$, 3.3 Hz, 2H), 3.62 (d, $J = 11$ Hz, 2H), 4.26 (td, $J = 9.8$, 1.8 Hz, 2H).

$Rh(PPh_3)_2(CO)Cl$ and NMMO: Reaction with Added Chloride. The procedure followed was the same as that described above, except that 0.5 mL of 20 mM bis(triphenylphosphoranylidene)ammonium chloride ([PPN][Cl]) was added to the solution of **2** and Ph_3P. The CO pressure was 800 Torr, and the Ph_3P concentration was 1.25 mM. No significant kinetic effect of added chloride was observed.

Kinetics of $Rh(PPh_3)_2(CO)Cl$-Catalyzed Deoxygenation of (p-$CH_3OC_6H_4)_2SeO$ (An_2SeO). Authentic An_2Se was prepared by the thiourea dioxide reduction of An_2SeO by the method of Lang.[42] ^1H NMR: An_2SeO: δ 3.79 (s, 3 H), 6.94 (d, $J = 8$ Hz, 2H), 7.56 (d, $J = 8$ Hz, 2H). An_2Se: δ 3.76 (s, 3 H), 6.79 (d, $J = 8$ Hz, 2H), 7.38 (d, $J = 9$ Hz, 2H). The only band in the IR spectrum of (p-$CH_3OC_6H_4)_2$SeO not overlapping with (p-$CH_3OC_6H_4)_2Se$ or not obscured by the solvent was at 1062 cm^{-1}. Disappearance of this band was used for kinetic data.

Control Reaction: An_2SeO and 1. An_2SeO (30.9 mg, 0.1 mmol) was dissolved in 5 mL of 1 mM **1** in dichloroethane under an argon atmosphere. No decrease in the amount of An_2SeO or **1**, or formation of CO_2, was detected by IR spectroscopy after 20 h at room temperature.

Control Reaction: An_2SeO and PPh_3. A solution of 20 mM each of PPh_3 and An_2SeO was prepared in dichloroethane. This was divided into two reaction cells, one of which was exposed to the atmosphere for 2 min while the other was left in the glovebox. After 6.3 h, the reaction exposed to the atmosphere revealed 15% of the starting An_2SeO to be present. After 6.8 h, the solution kept in the glovebox revealed 88% of the starting An_2SeO to be present. In the sample exposed to the atmosphere, a peak was growing in as a shoulder at ca. 1200 cm^{-1}, ν_{PO} for Ph_3PO.

Kinetics of 2-Catalyzed NMMO Deoxygenation. The experimental procedure for the kinetic runs is the same as that used for the rhodium-catalyzed runs, with the exception that the samples were purged with argon for 2 min at 0 °C to remove the CO in solution and to convert the $Ir(PPh_3)_2(CO)_2Cl$ to $Ir(PPh_3)_2(CO)Cl$. Due to evaporation of the solvent during purging, all An_2SeO absorbances were normalized to the absorbance for $Ir(PPh_3)_2(CO)Cl$. Because the rates were combinations of both a zero-order term and a first-order term, both first-order and zero-order observed rate constants were calculated.

Control Reaction: $Ir(PPh_3)_2(CO)Cl$ and NMMO in the Absence of CO. A 2 mM dichloroethane solution of $Ir(PPh_3)_2(CO)Cl$ (4.2 mL) was added to 0.1 mmol of NMMO; the resulting NMMO concentration was 24 mM. The reaction mixture was kept at room temperature in a vial in the glovebox. After 24 h, 78% of the $Ir(PPh_3)_2(CO)Cl$ remained, calculated from ν_{CO} at 1964 cm^{-1}. Sixty three percent of the NMMO remained, based on the IR band at 1170 cm^{-1}. No CO_2 was detectable in the IR spectrum. ^{31}P NMR revealed that Ph_3PO was being produced. The integration of the signals showed the total phosphorus to be 23% Ph_3PO, 77% $Ir(PPh_3)_2(CO)Cl$. While these results show a degradation of the $Ir(PPh_3)_2(CO)Cl$ and NMMO with time, this occurred over 24 h at room temperature. This is not expected to be significant under the experimental conditions, where the run times are shorter (less than ca. 4 h), the temperature is 0 °C, and there is only a small amount of $Ir(PPh_3)_2(CO)Cl$ present in solution. Of greater importance is the observation that no detectable CO_2 was produced, suggesting that oxygen transfer to coordinated CO is not taking place.

$Ir(PPh_3)_2(CO)Cl$ and NMMO under 800 Torr of CO: NMR Identification of Products. Conditions for this reaction were identical with those used for kinetic studies, with the exception that the solvent used was $CDCl_3$ (1 mM $Ir(PPh_3)_2(CO)Cl$, 800 Torr of CO, 20 mM NMMO). After 1.5 h, IR spectroscopy revealed CO_2 (ν_{asym} 2337 cm^{-1}) and $Ir(PPh_3)_2(CO)_2Cl$ (ν_{CO} 1984, 1930 cm^{-1}). ^1H NMR spectroscopy revealed only NMM: δ 2.27 (s, N−CH_3, 3 H), 2.39 (t, 4 H), 3.70 (t, 4 H). The ^{31}P NMR spectrum showed a singlet at approximately 9.74 ppm ($Ir(PPh_3)_2(CO)_2Cl$).

Kinetics of $Ir(PPh_3)_2(CO)Cl$-Catalyzed Deoxygenation of Selenium Oxides. Kinetic runs were performed as described above, with samples purged with argon for 2 min and the absorbance normalized to the absorbance for $Ir(PPh_3)_2(CO)Cl$. The disappearance of the peak at 1062 cm^{-1} in the IR spectrum of An_2SeO was monitored for kinetic runs. The end point at this wavelength was measured at the completion of the kinetic runs—the value was usually 0.010. This was subtracted from the measured absorbance for each data point. The disappearance of Ph_2SeO was monitored by IR spectroscopy at 834 cm^{-1}; the absorbance at this wavelength was zero when the reactions were complete.

Control Reaction: $Ir(PPh_3)_2(CO)Cl$ and An_2SeO in the Absence of CO. A solution of 2 mM $Ir(PPh_3)_2(CO)Cl$ (5 mL) was added to 0.1 mmol An_2SeO. After 19.5 h at room temperature, there was no decrease in the An_2SeO absorbance at 1062 cm^{-1}, no decrease in the ν_{CO} band of $Ir(PPh_3)_2(CO)Cl$ (1964 cm^{-1}), and no CO_2 was detected ($\nu_{asym} = 2340$ cm^{-1}).

$Ir(PPh_3)_2(CO)Cl$ and An_2SeO under CO—Product Identification. This reaction was run under the same conditions as those used for the kinetic runs, with the exception that $CDCl_3$ was used as the solvent. After 24 h at room temperature, the IR spectrum showed CO_2 at 2337

(42) Comasetto, J.; Lang, E. *J. Organomet. Chem.* **1987**, *334*, 329−340.

cm^{-1} and $Ir(PPh_3)_2(CO)_2Cl$, $\nu_{CO} = 1984, 1930\ cm^{-1}$. The absorbance at 1062 cm^{-1} was 0.010. ^1H NMR spectroscopy revealed δ 3.77 (s, $-OCH_3$, 3 H), 6.79 (d, $J = 9$ Hz, 2 H), and 7.38 (d, $J = 9$ Hz, 2 H), consistent with a complete conversion to An_2Se. ^{31}P NMR spectroscopy revealed a singlet, δ 9.48, attributable to $Ir(PPh_3)_2(CO)_2Cl$.

$Ir(PPh_3)_2(CO)Cl$ and Ph_2SeO under CO—Product Identification. After 24 h at room temperature, the formation of CO_2 (2337 cm^{-1}) and $Ir(PPh_3)_2(CO)_2Cl$, ($\nu_{CO} = 1984, 1930\ cm^{-1}$) was observed. The Ph_2SeO absorbance at 834 cm^{-1} had completely disappeared. ^1H NMR spectroscopy revealed two multiplets at δ 7.27 and 7.47 consistent with complete conversion to Ph_2Se as compared with a commercially obtained sample.

Kinetics of the Reaction of $[Ir(PPh_3)_2(CO)_3][BPh_4]$ with An_2SeO. A 2 mM stock solution of $[Ir(PPh_3)_2(CO)_3][BPh_4]$ in acetone-d_6 (0.6 mL) was placed in a resealable NMR tube. The sample was then placed under 2 atm of CO. After the NMR sample was frozen in liquid nitrogen, 0.2 mL of a 40 mM stock solution of the selenium oxide in acetone-d_6 was quickly added via syringe. The sample was then evacuated, and 2 atm of fresh CO was added to the sample. The sample was then maintained at -78 °C while mixing, and then placed in the probe of the NMR spectrometer at the appropriate temperature. The reaction was followed by ^1H NMR spectroscopy by monitoring the methoxy resonances of the anisolyl groups.

Reaction of $[Ir(PPh_3)_2(CO)_3][BPh_4]$ with Ph_3AsO. The cationic iridium carbonyl was prepared by a literature procedure.[18] Two bands were observed in the metal carbonyl region of the IR spectrum, $\nu_{CO} = 2015\ cm^{-1}$, and a weak absorption at 2075 cm^{-1} in dichloroethane. The ^{31}P NMR spectrum revealed a singlet δ -2.86. One milliliter of a solution containing 5 mM $[Ir(PPh_3)_2(CO)_3][BPh_4]$ and 10 mM Ph_3AsO in diglyme was measured into a 2-mL cell equipped with a Kontes high-vacuum valve and a septum inlet. CO (800 Torr) was added to the evacuated cell following 2 freeze−pump−thaw cycles. $[Ir(PPh_3)_2(CO)_3][BPh_4]$ and CO_2 concentrations were analyzed by IR spectroscopy at 2008 and 2337 cm^{-1}, respectively. Ph_3As was monitored by GC analysis by using a HP-1 methyl silicone column: 25 M × 0.25 mm, 0.5 μM film. The IR spectrum after 50 h at 50 °C revealed several unidentified peaks (cm^{-1} (absorbance)): 2048 (0.019); 1988 (0.239); 1969 (0.350); 1930 (0.151). No peak was detectable at 2008 cm^{-1}.

Preparation of *cis*-$Pt(Ph_3As)(CO)Cl_2$, 3. To a suspension of 100 mg of $PtCl_2$(1,5-cyclooctadiene) in 5 mL of dichloromethane was added 800 Torr of CO, producing a pink suspension upon stirring. To this suspension was added 80 mg (1 equiv) of Ph_3As in 5 mL of dichloromethane. Upon addition of the Ph_3As, the solution turned to pale yellow. The solvent was removed in vacuo, and the crude product was recrystallized from dichloromethane giving 130 mg of **3** (80% yield).

Deoxygenation Reactions of *cis*-$Pt(Ph_3As)(CO)Cl_2$, 3. Solutions of **3** in dichloromethane (5−10 mM) with added Ph_3AsO (100−200 mM) were placed under CO atmosphere. Upon standing, these solutions turned various shades of green. The IR spectra of the solutions displayed peaks indicative of platinum carbonyl anions (ca. 2060, 1860 cm^{-1}), or peaks due to an uncharacterized species (2055, 2045 cm^{-1}). Thermolysis of these samples at 90 °C resulted in the regeneration of **3** as observed by IR spectroscopy and a return to a pale yellow solution. The complete conversion to Ph_3As was confirmed by gas chromatography, while the formation of CO_2 was confirmed by IR spectroscopy. After catalysis was complete, additional Ph_3AsO was added and the cycle repeated up to three times (for a total of 60 turnovers), still regenerating **3** as the sole organometallic species.

Acknowledgment. We thank the Division of Chemical Sciences, Office of Basic Energy Sciences, Office of Energy Research, U. S. Department of Energy for support of this work. A. S. G. thanks the Camille and Henry Dreyfus Foundation for a Teacher Scholar Award and the Alfred P. Sloan Foundation for a Research Fellowship. Prof. Steven Nolan is thanked for communication of unpublished results.

JA970158S